Synthesis of concentrated aqueous dispersions of reduced graphene oxide

R. TARCAN[1], M. HANDREA-DRAGAN[1], I. BOTIZ[1,2,*]
[1]*Interdisciplinary Research Institute in Bio-Nano-Sciences, Babes-Bolyai University, 400271 Cluj-Napoca, Romania*
[2]*Department of Physics of Condensed Matter and Advanced Technologies, Faculty of Physics, Babeș-Bolyai University, 400084 Cluj-Napoca, Romania*

Reduced graphene oxide (RGO) is an excellent substitute for pristine graphene thanks to its outstanding optical, electrical, and thermal properties. However, a significant challenge remains: the ability to stabilize RGO in aqueous dispersions. This paper proposes a potential method for obtaining stable RGO dispersions in water in rather high concentrations, by using microwave-assisted hydrothermal reduction of graphene oxide in the presence of hydrazine hydrate and ammonia. While UV-vis and Raman analysis confirm the success of the reduction reaction, the dynamic light scattering further shows how centrifugation speed influences the RGO flake size distribution in resulting water dispersions. Furthermore, uniform and homogeneous RGO thin films could be obtained from concentrated water dispersions of RGO by simply employing the spin-coating technique. Fabricating such films from typically diluted RGO water dispersions is highly challenging.

(Received July 19, 2024; accepted October 7, 2024)

Keywords: Reduced graphene oxide, Dispersion, Microwave-assisted hydrothermal synthesis

1. Introduction

Reduced graphene oxide (RGO) is one of graphene's derivatives and it presents a basal plane made of sp^2-hybridized carbon atoms disposed in a honeycomb lattice, exhibiting structural defects and decorated with oxygen functional groups. RGO is a great substitute for pristine graphene, mainly due to its similar properties to those of graphene. RGO can be synthesized through top-down methods that are more facile and more cost-effective compared to the bottom-up ones, offering a wide range of options regarding the processability of the resulting product. However, one of the biggest challenges remains the ability to produce graphene or RGO in high quantities. In order to do so, it is crucial to understand the dispersibility and solution processability of RGO, which in turn will make RGO practical even for more applications.

RGO is usually synthesized from graphene oxide (GO) through a reduction process which removes some of the oxygen-containing groups from the graphene sheets and partially restores the sp^2-hybridized carbon network. Therefore, the structure of RGO exhibits a complex surface chemistry, characterized by the existence of hydrophobic sp^2 carbon domains and hydrophilic oxygen-containing groups. This is the reason why it is rather challenging to achieve good dispersibility of RGO in water. Graphene-based materials have the tendency to agglomerate and form aggregates in aqueous solutions because of the Van der Waals interactions occurring between the graphitic sheets. This tendency can be restrained using proper strategies which can improve the dispersibility of RGO, such as covalent [1, 2] or non-covalent functionalization [3, 4], surfactant-assisted dispersion [5, 6], and stabilization with polymers [7, 8] or other materials [9-11]. Having RGO in stable dispersions in water comes with multiple advantages: it enables its integration in various aqueous systems which can be further processed into different composites, coatings, or thin films, thus opening new possibilities to explore its unique properties towards a plethora of technological [12] and biomedical applications [13-15].

Even though various ways have been explored in order to obtain stable dispersions of RGO in water, the inclusion of external stabilizers is undesirable in the majority of applications, mainly because they may be difficult to remove or can deteriorate RGO's properties and consequently diminish the performance of the resulting composites or devices. While it is well known that GO is able to form well-dispersed aqueous colloids [16, 17] thanks to its increased hydrophobicity given by the presence of oxygen-containing groups on its basal plane, Li and co-workers [18] have shown that while dispersed in water, GO sheets are negatively charged, as a result of ionization of the carboxylic and phenolic hydroxylic groups [19, 20]. Hence, the formation of stable GO colloids in water is dependent on hydrophilicity and electrostatic repulsion. Given that the carboxylic groups are not reduced by hydrazine hydrate [21], they will still be present on the surface of the RGO, and thus they should still be charged in aqueous dispersions.

Li et al. [18] suggested an ingenious method to stabilize RGO dispersions in water without the aid of any stabilizing agents or functionalization, but simply through rigorous control of pH, electrolyte concentration, and the content of dispersed particles. In their experimental approach, graphite oxide, previously synthesized through modified Hummers method [22], was dispersed in water in a concentration of 0.05 wt.% followed by exfoliation through ultrasonication in order to obtain a stable dispersion of GO in water. Prior

to the reduction reaction, GO dispersion was centrifuged in order to remove the unexfoliated graphite oxide. The reduction agent was hydrazine hydrate in the presence of ammonia solution, and the optimal ratio of hydrazine to GO was 7:10. The reaction mixture was heated and stirred for 1 h at 95 °C in a water bath, leading to a stable dispersion of RGO in water. The important role of ammonia in this process was to generate a maximal charge density for RGO sheets and to favor the increase of the pH to ~10. Afterwards, ammonia could be easily removed from RGO-based thin films or composites due to its high volatility. Despite its increased toxicity, hydrazine hydrate acts as a reducing agent. Both hydrazine and ammonia dissociate in water, thus generating ionic species that act as electrolytes and maintain the dispersion stable. Additionally, the colloidal stability is also dependent on RGO concentration, as high concentrations lead to the flake formation and agglomeration of the graphitic sheets.

Later on, the method proposed by Li et al. was streamlined by Iliut et al. [23] while preparing RGO in order to enhance its fluorescence through non-covalent binding to riboflavin. They have replaced the traditional heating with the use of a microwave heating reactor, thus using a microwave-assisted hydrothermal reduction method. In their approach, GO was successfully reduced to RGO in 20 minutes by heating the GO dispersion at a temperature of 100 °C.

Both methods lead, however, to low concentrations of RGO in the final dispersion, below 0.05 mg/mL. Nonetheless, because the reduction of GO in water using hydrazine leads to RGO with electrical properties similar to a p-type semiconductor [24, 25], the resulting RGO can be a potential material for future applications in optoelectronics [14]. Moreover, it is possible for the above methods to be combined and optimized in order to obtain stable RGO dispersions in water in higher concentrations in order to enhance the material's properties and expand its applicability to, for instance, polymer-based composites. This study presents an investigation of how variations of GO, hydrazine and ammonia quantities in the reaction mixture can lead to stable dispersions of RGO in water in concentrations as high as 3 mg/mL.

2. Materials and methods

2.1. Materials and equipment

Graphite powder (325 mesh, 99.9995%) was sourced from Alfa Aesar. potassium permanganate and hydrazine hydrate solution 28% were purchased from Sigma-Aldrich; hydrogen peroxide 30%, ammonia solution 25%, sulfuric acid 95–97%, and acetone were acquired from Nordic Invest, while hydrochloric acid 37%, phosphoric acid 85%, and ethanol came from the Chemical Company.

An ultrasonication bath Elmasonic S 30 H was used for exfoliation of graphite oxide to graphene oxide in solution, and a Hettich Mikro 22 centrifuge was used to eliminate the unexfoliated graphite oxide from the solution. For the reduction reaction, a microwave-assisted reactor Anton Paar Monowave 300 has been used. The pH of the solutions was measured using a Metler Toledo pH-meter. GO and RGO were identified by UV-vis absorption spectroscopy, using a Jasco 630 Spectrophotometer, from diluted solutions of the as-prepared GO and RGO dispersions, while Raman spectroscopy confirmed the success of the reduction reaction (a Witec Alpha 300 RA confocal Raman Microscope was used for measurements). Further characterizations involved flake size distribution of RGO in aqueous dispersions by DLS technique, using a Malvern ZS90 instrument. Moreover, optical images of the RGO thin films were taken using an inverted microscope Carl Zeiss Axio Observer Z1, while for the acquisition of AFM images a system from Molecular Devices and Tools for Nano Technology (NT-MDT) fixed on an Olympus IX71 optical microscope was used in tapping mode. AFM measurements were performed using high resolution Noncontact Golden Silicon probes from NT-MDT. Probes possessed a tip radius of curvature smaller than 10 nm and a tip height of 14–16 μm and were Au coated on the detector side cantilever. The cantilever, of a length of 125 ± 5 μm, displayed a resonance frequency in the range of 187–230 kHz and a nominal force constant ranging between 1.45–15.1 N/m. AFM images (256 × 256 lines) were obtained using a scanning speed of around 2 μm/s and a set point of 10-12 V. The latter was adjusted so that a rather soft tapping regime is obtained.

Before their use, glass substrates utilized for RGO thin film depositions have been treated for 20 min with UV-Ozone by employing a Novascan PSD Pro cleaning system. Finally, for the deposition of thin films, a spin coater type Laurell WS-650MZ-23-NPPB was employed.

2.2. Graphene oxide synthesis and its dispersion in water

Improved Hummers method proposed by Marcano et al. [26, 27] was used in order to obtain graphite oxide. For this, graphite flakes (325 mesh, 99.9995%) were oxidated to graphite oxide using potassium permanganate ($KMnO_4$) and a mixture of concentrated sulfuric acid (H_2SO_4) and phosphoric acid (H_3PO_4). The reaction mixture was stirred at 50 °C for 12 h, followed by the addition of ice-cold ultrapure water and H_2O_2. The resulting precipitate was washed with diluted hydrochloric acid (HCl), ultrapure water, and ethanol, then dried using a vacuum desiccator at room temperature for up to few hours until the samples are completely dried, leading to a brown graphite oxide powder.

Afterwards, the as-obtained graphite oxide powder was dispersed in water in concentrations of 1 mg/mL and 5 mg/mL and sonicated for 1 h in order to promote exfoliation of graphite oxide to GO, followed by centrifugation for 30 min at 3000 rpm to eliminate the unexfoliated graphite oxide from the dispersion. The resulting supernatants containing stable dispersions of GO in water were further employed in different attempts to obtain stable dispersions of RGO in concentrations higher than 0.05 mg/mL.

2.3. Reducing graphene oxide in water

In order to perform the reduction of GO in water, a solution of hydrazine hydrate 25% and ammonia solution 28% were used. In an attempt to maintain a mass ratio of GO:N_2H_4 of 10:7 and a pH in the mixture of around 10, for each milligram of GO 44 µL of hydrazine hydrate solution 25% and 16 µL of ammonia solution 28% were used. Therefore, a GO solution of 1 mg/mL is expected to lead to RGO dispersed in water in concentrations of approximatively 0.5 mg/mL and 1 mg/mL, while GO solution of 5 mg/mL should lead to RGO dispersions of higher concentrations, such as 2 mg/mL or even 3 mg/mL.

For the reduction reaction, a microwave-assisted hydrothermal method has been employed. A mixture of GO dispersion in water, hydrazine hydrate and ammonia has been placed in a quartz tube and introduced in an Anton Paar Monowave 300 microwave reactor, where it was heated at 100 °C for 20 minutes. The quantities of each reactant are presented below in Table 1.

Table 1. Reactants quantities used for the reduction of GO to RGO in water, in concentrations of 0.5, 1, 2, and 3 mg/mL

Desired concentration of RGO dispersion in water (mg/mL)	GO 1 mg/mL (µL)	GO 5 mg/mL (µL)	Water (µL)	Hydrazine Hydrate 25% (µL)	Ammonia 28% (µL)	pH
0.5	500	n/a	500	22	8	10.7
1	1000	n/a	n/a	44	16	10.9
2	n/a	400	600	88	32	11.1
3	n/a	600	400	132	48	11.2

3. Results and discussion

3.1. Reduced graphene oxide dispersion in water

In order to reduce GO to RGO and stabilize it in water, different amounts of reducing agent have been used, as presented in Table 1. First confirmation of the successful reduction of GO to RGO was the change in dispersion's color noticed after the reaction. While the GO dispersion presents a light brown color, after the reduction its color changes to black, as an indication that the oxygen-containing groups have been removed, and that the sp^2 network is partially restored. Digital images of GO dispersion in water and its resulting RGO dispersions of 0.5, 1, 2, and 3 mg/mL are illustrated in Fig. 1a,c-f, along with an RGO dispersion in a concentration of only 0.05 mg/mL, synthesized using a method previously employed in our laboratory [23] (Fig. 1b). The latter is presented for comparison reasons, in order to illustrate from a qualitative point of view the increased concentration associated with a more opaque, darker color of RGO in the dispersions synthesized by the methods presented in this study. While the RGO dispersion of 0.5 mg/ml was stable and did not present any agglomeration right after the reduction, the RGO dispersions of 1, 2 and 3 mg/mL presented some aggregated RGO flakes that could be successfully removed after centrifugation at 10000 rpm for 30 min, as illustrated in Fig. 1g. Most probably the agglomeration of RGO flakes occurred in these dispersions because of the increased concentration of hydrophobic graphitic sheets interacting with each other through Van der Waals forces, but also due to the increasing pH value of the final dispersion (from 10.7 at 0.5 mg/mL to 11.2 at 3 mg/mL) with the increasing amounts of hydrazine and ammonia used in reaction. It is also possible that the electrolytes resulting from the dissociation of hydrazine and ammonia were in too low concentration or were not able to overcome the stacking between the graphitic sheets. It is important to mention that all RGO dispersions in water were stable only for relatively short periods of time, e.g. less than 24 h. Fortunately this period of time is enough to make use of the concentrated RGO dispersions in various technological applications. Moreover, for future characterizations, RGO dispersion of 2 mg/ml was selected, as our RGO synthesis method presented the highest reproducibility in this case.

In order to confirm the success of the reduction process, we have recorded the UV-vis spectra for both GO and RGO using a quartz cuvette of 1 mm (Fig. 2a). Due to the increased opacity of the dispersions, the spectra were recorded on diluted dispersions coming from stock dispersions of GO 5 mg/ml and RGO 2 mg/mL. Raman investigation also confirmed that GO was reduced in the final dispersions (in this case, the spectra were acquired on thin films deposited on quartz substrates by drop-casting) (Fig. 2b).

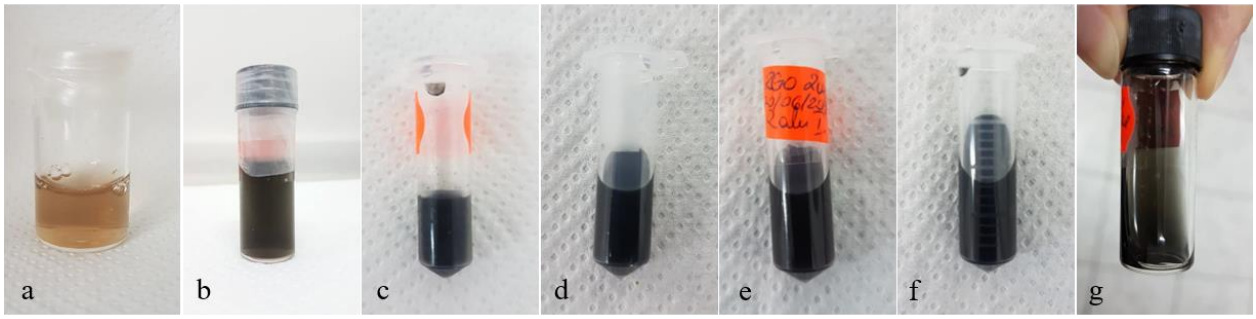

Fig. 1. (a-g) Digital photos of a GO dispersion in water (a) and RGO dispersions of 0.05 mg/mL (b), 0.5 mg/mL (c), 1 mg/mL (d), 2 mg/mL (e), 3 mg/mL (f), and 3 mg/mL (g) in water (color online)

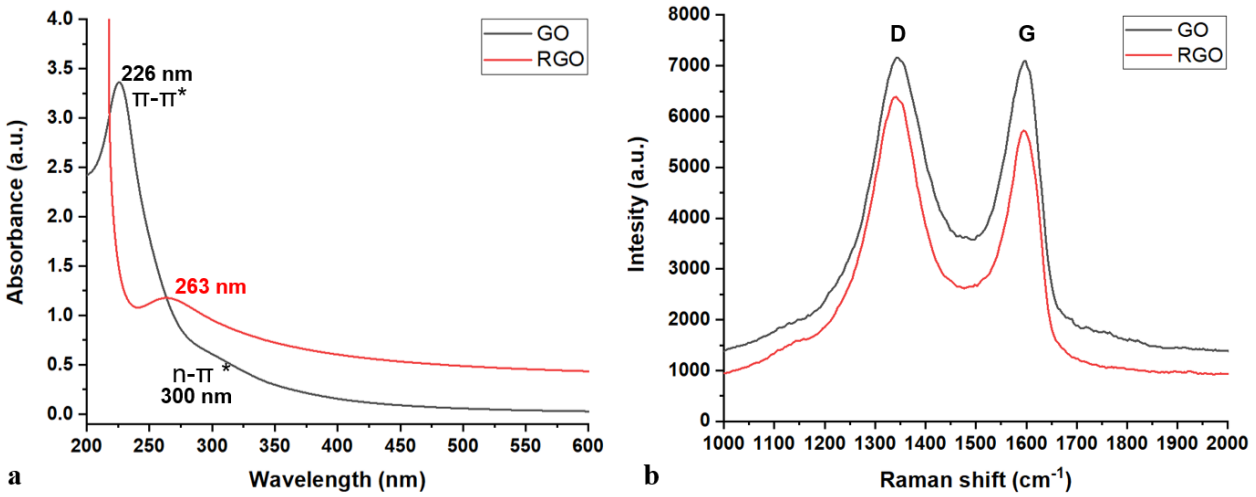

Fig. 2. (a) UV-vis and (b) Raman spectra of GO and RGO dispersions in water (color online)

The UV-vis spectra for GO exhibit characteristic peaks corresponding to GO's structural particularities. The peak maximum at ~226 nm is characteristic to π-π* transitions from C=C bonds present in the aromatic structure of the graphitic basal plane, while the shoulder visible at ~300 nm is a result of the n-π* transitions characteristic to C=O bonds from oxygen functional groups present on the structure of GO [28]. After the reduction reaction, not only that the color of the dispersion changed from brown to black, but the UV-vis spectrum was also different, suggesting that significant changes happened with GO during the reaction. Here, the maximum absorption peak characteristic for C=C bonds appeared redshifted to ~263 nm, the shoulder characteristic for C=O bonds completely disappeared, while the absorption has increased throughout the entire visible and NIR range. These changes suggest that the oxygen-containing groups have been partially removed, sp^3 sites became sp^2, thus leading to a restoration of the sp^2 network in the graphitic basal plane. These observed specifics are in line with the previously reported characteristics of graphene absorption spectra [29].

Raman spectra for GO and RGO presented two bands, D and G, characteristic for carbon structures. The D band offers information regarding the defects present in sp^2 network, and is, consequently, characteristic for the quality of the graphitic sheets [30, 31] (typically, the absence of D band in graphene-based materials indicates low defect content [32]), while the G band arises from the in-plane stretching vibrations of the C=C bonds [31, 33]. In GO spectra, the D band appeared at 1343 cm^{-1} and the G band was located at 1594 cm^{-1}, while in RGO the same bands appeared at 1340 cm^{-1} and 1595 cm^{-1}, respectively. Following the reduction of GO, the band width was narrower, and the I_D/I_G ratio increased from 1.01 in GO to 1.12 in RGO, suggesting the success of the reduction process with a partial restoration of the sp^2 conjugated network.

Further characterization of the RGO dispersions in water involved a brief study on how centrifugation influences the concentration and flake size distribution from a qualitative point of view. In this regard, RGO dispersions were centrifuged for 30 minutes at three different speeds: 4000 rpm, 8000 rpm, and 12000 rpm. The supernatants of these three dispersions were analyzed by UV-vis spectroscopy, and as expected, the decreasing absorbance indicated a decrease in RGO concentration with the increasing centrifugation speed (Fig. 3a). This confirmed that during centrifugation, the RGO flakes of increased size were removed and only the smaller flakes remained in the final dispersion (obviously, this process was accompanied by a slight reduction of the RGO concentration in the final dispersion). This result has been further confirmed by DLS

analysis (Fig. 3b), showing that at high centrifugation speeds not only that the big flakes were removed (according to previous reports [13], before centrifugation, RGO solutions are expected to also contain highly aggregated RGO structures of sizes reaching 8-10 micrometers), but there was a high probability that the RGO flakes were colliding, leading to flake fracture and thus resulting in a decrease in flake size.

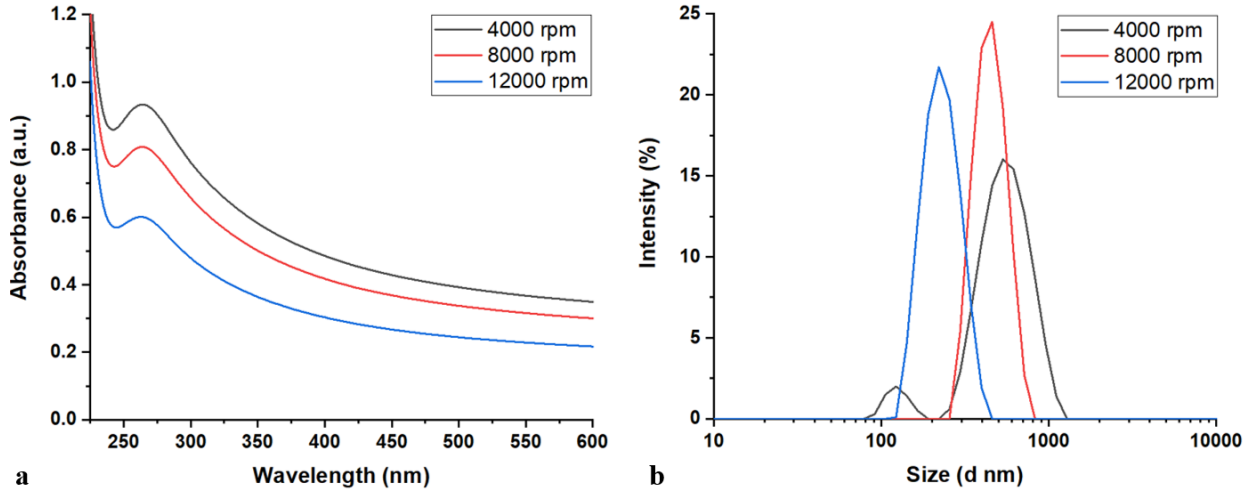

Fig. 3. (a-b) Influence of centrifugation speed on concentration and flake size distribution in RGO dispersions in water, characterized by UV-vis spectroscopy (a) and DLS (b) (color online)

3.2. Reduced graphene oxide thin films from water dispersions

There is a great potential of utilizing RGO in a plethora of applications [14], and in order to maximize this potential, it is important to have RGO that can be processed in both dispersions and thin films. Therefore, further investigation involved a simple study on thin films deposition from concentrated RGO aqueous dispersions using two well-known techniques, spin-casting and drop-casting, the final target being the generation of uniform and homogeneous RGO films. Convective self-assembly has also been used in an attempt to deposit RGO thin films from water dispersion, however, the increased concentration, hydrophobicity and strong Van der Waals interactions lead to the agglomeration of RGO flakes, making it impossible to obtain homogenous thin films. In thin film fabrication experiments we have used an RGO dispersion in water of 2 mg/mL and glass slides as substrates. Prior to any use, the substrates were firstly washed with water and acetone and then treated with UV-ozone for 20 minutes.

Depositing thin films by spin-coating from RGO aqueous dispersion presented great challenges. At high rotational speed, the RGO-containing aqueous droplet was instantaneously removed from the substrate, leaving a very small amount of solution on the substrate, leading to very thin, yet discontinued films with small flakes of RGO randomly distributed (Fig. 4a,b). At slow rotational speeds, the evaporation of water was also slow, and the increased hydrophobicity of RGO and the repetitive rotational movement lead to the agglomeration of the flakes (Fig. 4c,d). To overcome these fabrication issues, we have developed a spin casting procedure that started with slow rotations followed by gradual increase of the rotational speeds, while keeping the same spinning time for each step. The most uniform and homogeneous RGO films were obtained when 15 µL of RGO water dispersion were spun for 60 s at gradually increasing rotational speeds starting from 200 rpm to 1300 rpm (Fig. 4e,f). With such a recipe, the evaporation of water was appropriate and led to continuous, uniform films. However, it is important to mention that this method led to a random distribution of the RGO flakes without a specific organizational pattern corresponding to certain deposition parameters. Moreover, the experiments presented here provided no relevant information on the thickness of RGO flakes, but based on recent reports containing relevant transmission and scanning electron microscopy and AFM data, RGO flakes should be expected to display a multilayered structure comprised of more than ten RGO individual sheets [13].

Instead, drop-casting is a thin film deposition technique that involves the placement of a dispersion droplet on a substrate, followed by solvent evaporation at room or other temperatures of interest. In this case, the temperature at which drop-casting is proceeding dictates the rate of water evaporation and thus, strongly influences the morphology of the resulting RGO thin films. Therefore, in order to control this temperature, prior to drop-casting, all glass substrates were place on a heating plate of controlled temperature. As a result, the most uniform films have been obtained at room temperature and at 50 °C, as illustrated in Fig. 5a,b. Conducting drop-casting at higher temperatures, ranging between 80 and 200 °C led to RGO thin films displaying multiple defects induced by faster evaporation of water (Fig. 4c,d). It is worth mentioning that at temperatures higher than 100 °C (including 200 °C) the evaporation of water happened almost instantly, leading to even more serious structural defects and random aggregation of the flakes, making the resulting RGO films impractical for applications.

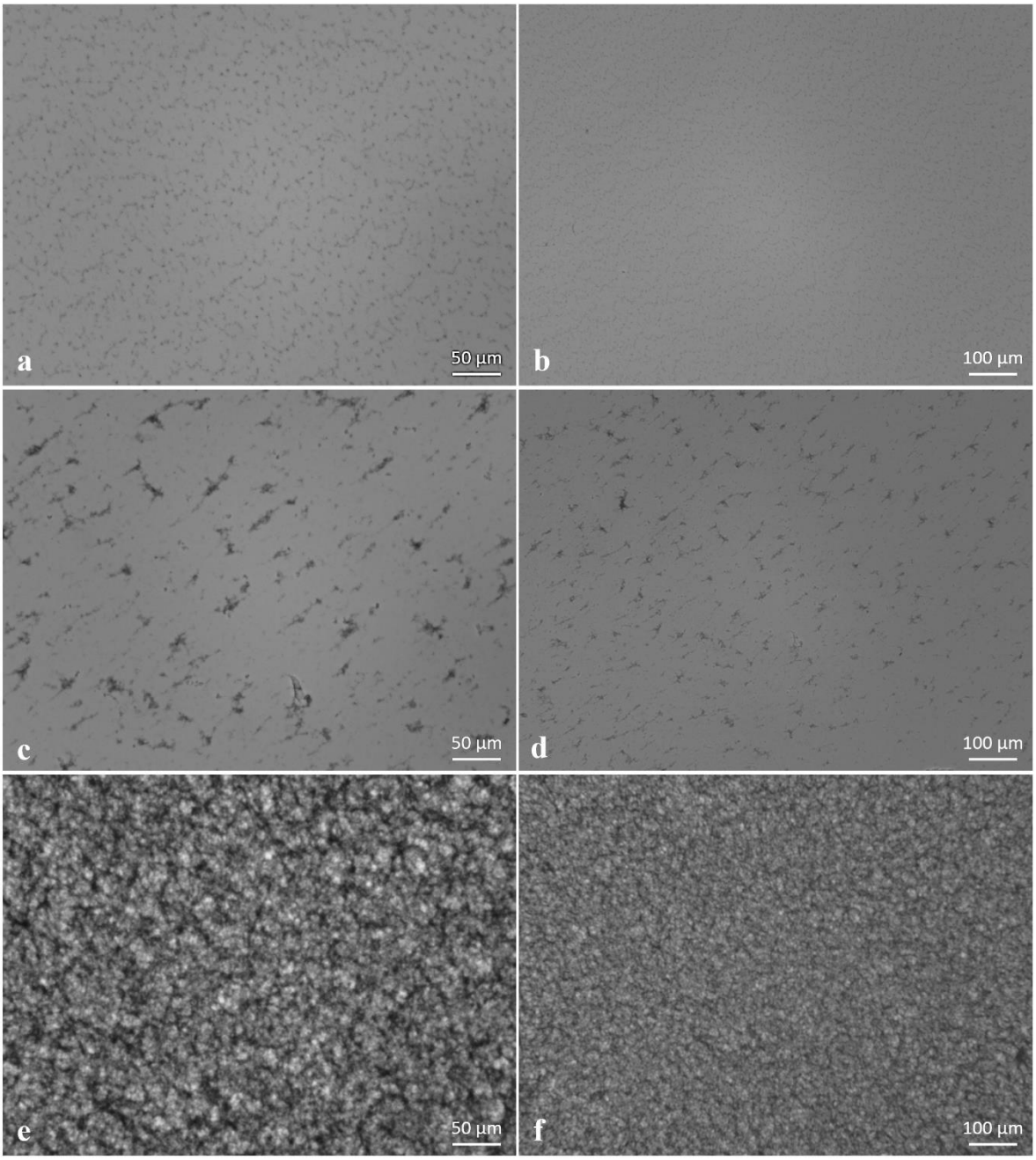

Fig. 4. (a-b) Optical micrographs of RGO thin films deposited by spin-coating at 1000 rpm for 60 s; (c-d) at 200 rpm for 300 s; (e-f) at rotational speeds increasing gradually from 200 rpm to 1300 rpm for 60 s each spinning step

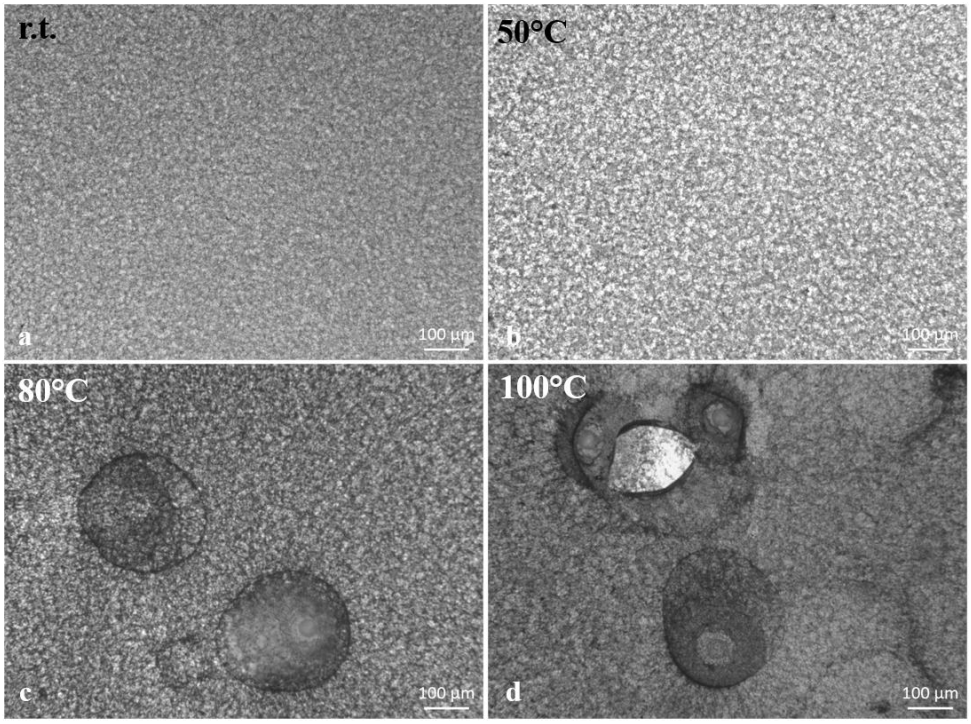

Fig. 5. (a) Optical images of RGO thin films deposited by drop-casting at: room temperature; (b) 50 °C; (c) 80 °C; (d) 100 °C

Analyzing the RGO thin films deposited by drop-casting at room temperature using the AFM technique, has confirmed their uniform morphology with some structural features randomly distributed, together with elongated, closely packed structures formed by the agglomeration of RGO flakes (Fig. 6). Additionally, the thickness of the RGO film, estimated by measuring the cross-sectional AFM profile of an intentional scratch performed on the film, has been approximated to several tens of nanometers (ranging between about 45 nm to roughly 65 nm).

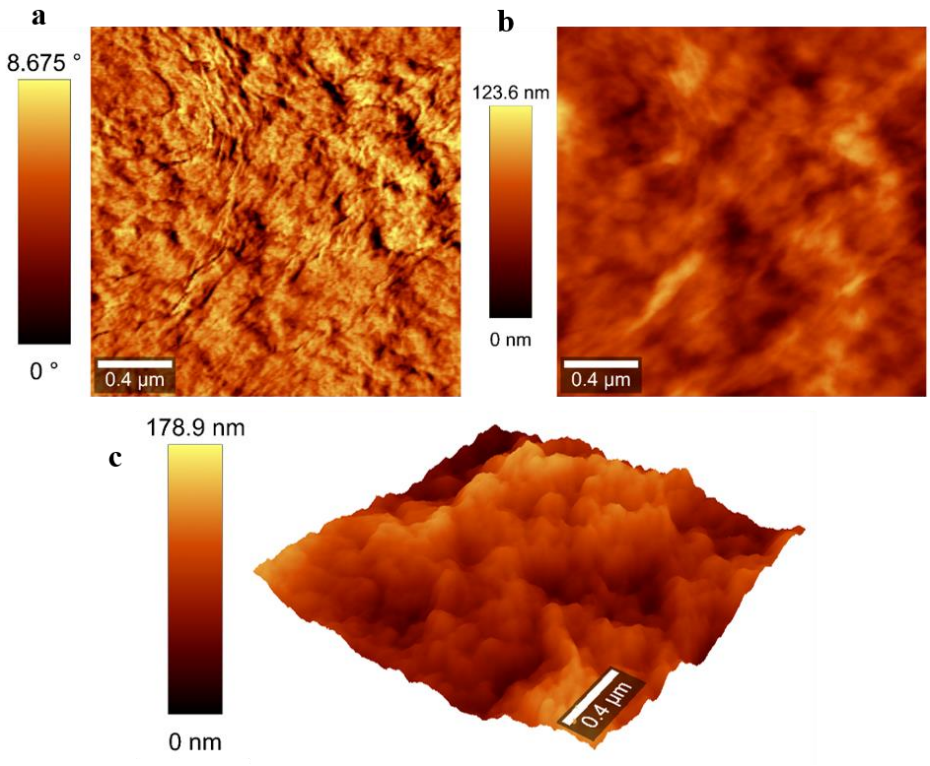

Fig. 6. (a)AFM height and (b) phase micrographs depicting the surface of an RGO film deposited by drop-casting at room temperature; (c) 3D representation of (a) (color online)

4. Conclusions

In this study we have shown that one can obtain stable RGO dispersions in water in concentrations higher than previously reported 0.05 mg/mL, using a microwave-assisted hydrothermal method to reduce GO in the presence of hydrazine and ammonia. Further characterizations of the RGO dispersion by UV-vis and Raman spectroscopies confirmed the success of the reduction reaction. Moreover, given the tendency or RGO to agglomerate and form flakes in water, we have investigated how centrifugation speeds have influenced the flake size distribution, concluding that at rotational speeds as high as 12000 rpm, not only that the bigger flakes were removed, but there was a high probability that the flakes were colliding, leading to their fracture and thus resulting in a decrease of the average flake size.

While it is important to be able to prepare stable dispersions of RGO in water, it is also detrimental to be able to process these dispersions as thin films and incorporate the obtained RGO in various composites. Therefore, we have also investigated the behavior of the RGO aqueous dispersions during the fabrication of thin films using spin-coating and drop-casting methods. We have observed that both methods led, only under specific processing conditions, to uniform, homogeneous film surfaces displaying random, often aggregated, RGO flakes. We believe these specific film processing conditions will be of interest to all researchers targeting to reproducibly fabricate uniform, high-quality RGO-based thin films.

Conflicts of interests

The authors declare that there are no conflicts of interest.

Acknowledgements

The authors acknowledge V. Ciobanas for preparing some initial RGO films and M. Potara for performing Raman investigations.

References

[1] C. Shan, H. Yang, D. Han, Q. Zhang, A. Ivaska, L. Niu, Langmuir **25**, 12030 (2009).
[2] H. Yang, C. Shan, F. Li, D. Han, Q. Zhang, L. Niu, Chemical Communications **26**, 3880 (2009).
[3] J. Guo, L. Ren, R. Wang, C. Zhang, Y. Yang, T. Liu, Composites Part B: Engineering **42**, 2130 (2011).
[4] D. Parviz, S. Das, H. S. T. Ahmed, F. Irin, S. Bhattacharia, M. J. Green, ACS Nano **6**, 8857 (2012).
[5] M. Lotya, Y. Hernandez, P. J. King, R. J. Smith, V. Nicolosi, L. S. Karlsson, F. M. Blighe, S. De, Z. Wang, I. T. McGovern, G. S. Duesberg, J. N. Coleman, Journal of the American Chemical Society **131**, 3611 (2009).
[6] M. Lotya, P. J. King, U. Khan, S. De, J. N. Coleman, ACS Nano **4**, 3155 (2010).
[7] A. B. Bourlinos, V. Georgakilas, R. Zboril, T. A. Steriotis, A. K. Stubos, C. Trapalis, Solid State Communications **149**, 2172 (2009).
[8] S. Das, A. S. Wajid, J. L. Shelburne, Y.-C. Liao, M. J. Green, ACS Applied Materials & Interfaces **3**, 1844 (2011).
[9] S. Lee, J.-S. Yeo, J.-M. Yun, D.-Y. Kim, Optical Materials Express **7**, 2487 (2017).
[10] J. Li, G. Xiao, C. Chen, R. Li, D. Yan, Journal of Materials Chemistry A **1**, 1481 (2013).
[11] T. Jiang, L. Maddalena, J. Gomez, F. Carosio, A. Fina, Polymers **14**(19), 4165 (2022).
[12] A. Petris, I. C. Vasiliu, P. Gheorghe, A. M. Iordache, L. Ionel, L. Rusen, S. Iordache, M. Elisa, R. Trusca, D. Ulieru, S. Etemadi, R. Wendelbo, J. Yang, K. Thorshaug, Nanomaterials **10**, 1638 (2020).
[13] R. Tarcan, M. Handrea-Dragan, O. Todor-Boer, I. Petrovai, C. Farcau, M. Rusu, A. Vulpoi, M. Todea, S. Astilean, I. Botiz, Synthetic Metals **269**, 116576 (2020).
[14] R. Tarcan, O. Todor-Boer, I. Petrovai, C. Leordean, S. Astilean, I. Botiz, Journal of Materials Chemistry C **8**, 1198 (2020).
[15] A. Zubarev, M. Cuzminschi, A.-M. Iordache, S.-M. Iordache, C. Rizea, C. E. A. Grigorescu, C. Giuglea, Diagnostics **12**, 2593 (2022).
[16] N. A. Kotov, I. Dékány, J. H. Fendler, Advanced Materials **8**, 637 (1996).
[17] T. Szabó, A. Szeri, I. Dékány, Carbon **43**, 87 (2005).
[18] D. Li, M. B. Müller, S. Gilje, R. B. Kaner, G. G. Wallace, Nature Nanotechnology **3**, 101 (2008).
[19] T. Szabó, O. Berkesi, P. Forgó, K. Josepovits, Y. Sanakis, D. Petridis, I. Dékány, Chemistry of Materials **18**, 2740 (2006).
[20] A. Lerf, H. He, M. Forster, J. Klinowski, The Journal of Physical Chemistry B **102**, 4477 (1998).
[21] S. Stankovich, D. A. Dikin, R. D. Piner, K. A. Kohlhaas, A. Kleinhammes, Y. Jia, Y. Wu, S. T. Nguyen, R. S. Ruoff, Carbon **45**, 1558 (2007).
[22] W. S. Hummers, Jr., R. E. Offeman, Journal of the American Chemical Society **80**, 1339 (1958).
[23] M. Iliut, A.-M. Gabudean, C. Leordean, T. Simon, C.-M. Teodorescu, S. Astilean, Chemical Physics Letters **586**, 127 (2013).
[24] S. Gilje, S. Han, M. Wang, K. L. Wang, R. B. Kaner, Nano Letters **7**, 3394 (2007).
[25] C. Gómez-Navarro, R. T. Weitz, A. M. Bittner, M. Scolari, A. Mews, M. Burghard, K. Kern, Nano Letters **7**, 3499 (2007).
[26] D. C. Marcano, D. V. Kosynkin, J. M. Berlin, A. Sinitskii, Z. Sun, A. Slesarev, L. B. Alemany, W. Lu, J. M. Tour, ACS Nano **4**, 4806 (2010).
[27] D. C. Marcano, D. V. Kosynkin, J. M. Berlin, A. Sinitskii, Z. Sun, A. S. Slesarev, L. B. Alemany, W. Lu, J. M. Tour, ACS Nano **12**, 2078 (2018).
[28] S. Saxena, T. A. Tyson, S. Shukla, E. Negusse,

H. Chen, J. Bai, Applied Physics Letters **99**, 013104 (2011).
[29] K. F. Mak, L. Ju, F. Wang, T. F. Heinz, Solid State Communications **152**, 1341 (2012).
[30] A. Kaniyoor, S. Ramaprabhu, AIP Advances **2**, 032183 (2012).
[31] R. Kumar, B. R. Mehta, M. Bhatnagar, R. S. S. Mahapatra, S. Salkalachen, P. Jhawar, Nanoscale Research Letters **9**, 349 (2014).
[32] C. Banciu, M. Lungulescu, A. Bara, L. Leonat, A. Teisanu, Optoelectron. Adv. Mat. **11**, 368 (2017).
[33] A. C. Ferrari, Solid State Communications **143**, 47 (2007).

*Corresponding author: ioan.botiz@ubbcluj.ro